

In Vivo Visualization of Perforating Vessels and Focal Scleral Ectasia in Pathological Myopia

Alexandre Pedinielli, Eric H. Souied, Francois Perrenoud, Nicolas Leveziel, Violaine Caillaux, and Giuseppe Querques

Department of Ophthalmology, Hopital Intercommunal de Creteil, University Paris Est Creteil, France

Correspondence: Giuseppe Querques, Department of Ophthalmology, University of Paris Est Creteil, Centre Hospitalier Intercommunal de Creteil, 40 Avenue de Verdun, 94010 Creteil, France; giuseppe.querques@hotmail.it.

Submitted: August 3, 2013

Accepted: September 26, 2013

Citation: Pedinielli A, Souied EH, Perrenoud F, Leveziel N, Caillaux V, Querques G. In vivo visualization of perforating vessels and focal scleral ectasia in pathological myopia. *Invest Ophthalmol Vis Sci*. 2013;54:7637–7643. DOI:10.1167/iovs.13-12981

PURPOSE. To describe focal scleral ectasia in areas of macular/perimacular patchy chorioretinal atrophy secondary to pathologic myopia.

METHODS. Thirty-nine consecutive patients with pathologic myopia and chorioretinal atrophy in at least one eye, with and without focal scleral ectasia, were analyzed by infrared reflectance (IR) and/or multicolor imaging, enhanced depth imaging optical coherence tomography (EDI-OCT) (39 patients, 78 eyes), and swept source (SS)-OCT (13 out of 39 patients, 26 eyes) cross-sectional scan.

RESULTS. Focal scleral ectasia was found in 12 out of 68 eyes (11 out of 39 consecutive patients, 27 females/12 males; mean age 65.7 ± 11.9 years) with macular/perimacular patchy chorioretinal atrophy, and was always observed inferior or temporal to the macula (mean 1.25 ± 0.38 /eye). Focal scleral ectasia, appearing on fundus examination as a deep dark round/oval lesion with well-defined borders, was characterized on EDI-OCT and SS-OCT by an abrupt posterior bow of the sclera with different degrees of scleral schisis on its borders. The retinal pigment epithelium and the choroid were absent in all lesions. IR reflectance and multicolor imaging showed large vessels that seem to emerge from the focal scleral ectasia, and crossing the area of patchy atrophy. EDI-OCT and SS-OCT revealed retrobulbar vessels perforating the sclera at the borders/bottom of the abrupt posterior bow of the sclera (i.e., focal scleral ectasia) and running through the superficial scleral thickness for the whole extension of the atrophic area.

CONCLUSIONS. We showed that perforating vessels are localized at the border/bottom of focal scleral ectasia in pathologic myopia.

Keywords: atrophy, choroid, enhanced depth imaging, macular degeneration, myopia, multimodal imaging, optical coherence tomography, perforating vessels, scanning laser ophthalmoscope, sclera

High myopia is a major cause of vision impairment and its prevalence has rapidly increased in the past 50 years.¹ High myopia accompanied by characteristic degenerative changes in the sclera, choroid, and retina, with compromised visual function, is generally referred to as pathologic myopia.² In pathologic myopia, excessive elongation and deformation of the eye may lead to the development of macular lesions, including posterior staphyloma, lacquer cracks, myopic choroidal neovascularization (CNV), myopic macular retinoschisis, and myopic chorioretinal atrophy.^{3–5}

Macular/perimacular patchy chorioretinal atrophy (a grayish-white lesion with well-defined borders), which is believed to be caused by a complete loss of the choriocapillaris and the subsequent degeneration of the photoreceptors and the RPE, may enlarge and cause central vision loss in patients with pathologic myopia due to foveal involvement.⁶

In macular/perimacular patchy chorioretinal atrophy, by means of enhanced depth imaging optical coherence tomography (EDI-OCT), we recently detected peculiar changes in the sclera of pathologic myopia eyes, characterized by focal ectasia and schisis (Querques G, unpublished observations, 2013). With EDI-OCT, deep choroidal images are enhanced by taking an inverted image and multiple B-scan averaging to improve the

signal-to-noise ratio.⁷ Retrobulbar structures can also be visible when the choroid is thin or absent, which is the case in pathologic myopia.⁸

The purpose of this study was to describe and interpret focal scleral ectasia detected in areas of macular/perimacular patchy chorioretinal atrophy secondary to pathologic myopia.

METHODS

Thirty-nine patients with pathologic myopia and macular/perimacular patchy chorioretinal atrophy in at least one eye that consecutively presented in the Department of Ophthalmology at the Hôpital Intercommunal de Créteil (Créteil, France) from January 2012 to March 2013 were studied. Our study was performed in agreement with French bioethical legislation and the Declaration of Helsinki for research involving human subjects. French Society of Ophthalmology Institutional Review Board approval was obtained for this study. The definition of pathologic myopia was a refractive error (spherical equivalent) >-8.00 diopters (D) or an axial length >26.5 mm, accompanied by characteristic degenerative changes in the sclera, choroid, and retina, with compromised visual

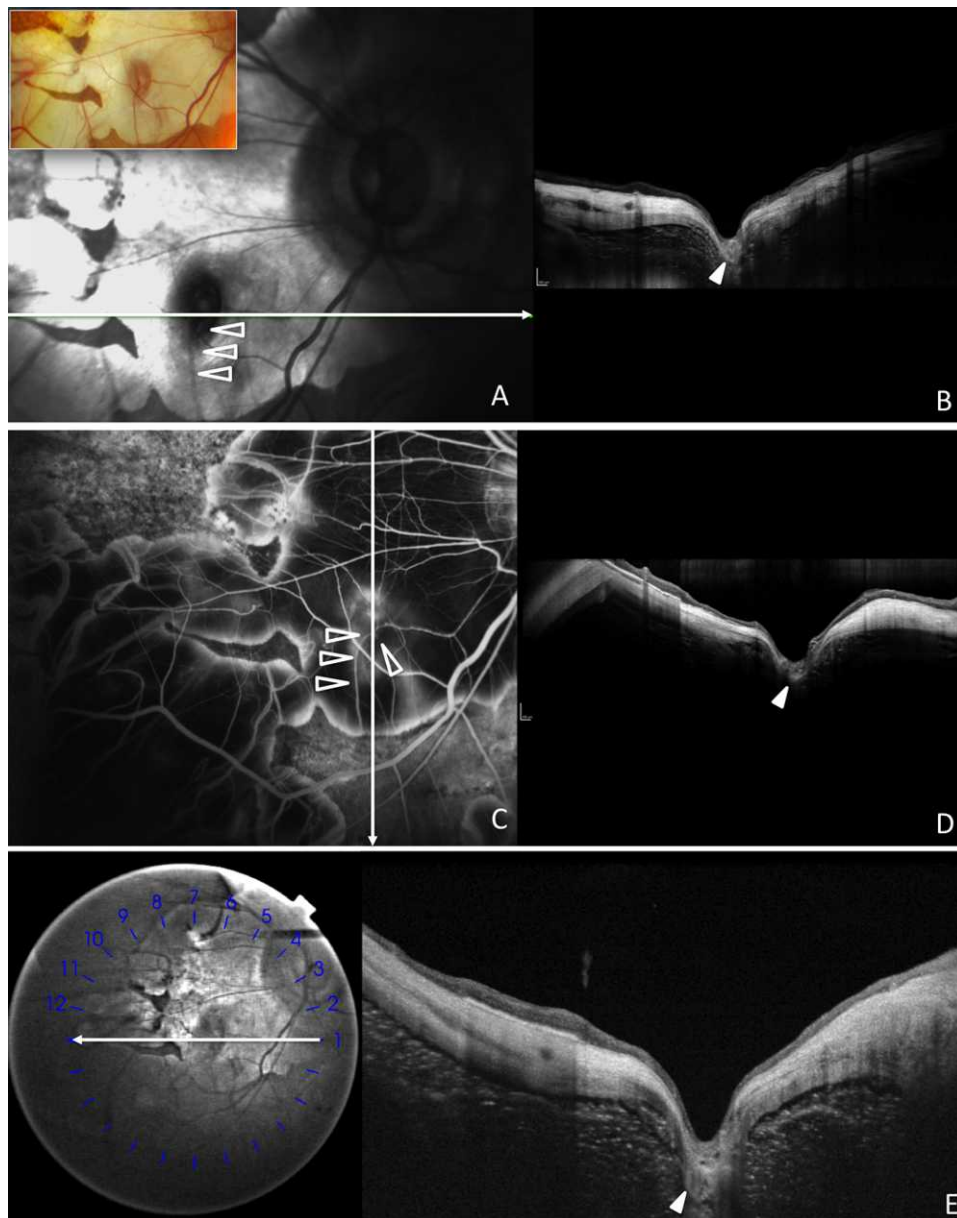


FIGURE 1. Color fundus photograph, IR, FA, EDI-OCT, and SS-OCT scan of a 78-year-old woman with high myopia. Infrared reflectance shows focal scleral ectasia as deep, dark round/oval lesions with well-defined borders surrounded by the atrophy crossed by a vessel ([A], *open arrowheads*). Note, on color fundus photograph, large vessels that seem to emerge from the deep dark round/oval lesion. Corresponding EDI-OCT scan shows the presence of a focal scleral ectasia (B). On FA, a crossing vessel is visible through the atrophic lesion ([C], *open arrowheads*). EDI-OCT (B, D) and SS-OCT (E) scans show the vessel at the bottom of the ectasia (*white arrowheads*).

function. All patients underwent a complete ophthalmic evaluation, including assessment of distance best-corrected visual acuity (BCVA) using Early Treatment Diabetic Retinopathy Study (ETDRS) charts, slit-lamp biomicroscopy, indirect fundus ophthalmoscopy, measurements of the axial length with an optical biometer (IOLMaster; Carl Zeiss Meditec, Dublin, CA), fundus biomicroscopy, confocal scanning ophthalmoscope (cSLO) multicolor images (MultiColor – Scanning Laser Imaging; Heidelberg Engineering, Heidelberg, Germany; an overlay of three distinctive cSLO wavelengths: blue reflectance [486 nm], green reflectance [518 nm], and infrared (IR) reflectance [815 nm]) and/or IR reflectance (19 out of 39 patients, and 39 out of 39 patients, respectively), and spectral domain (SD)-OCT (Spectralis HRA-OCT; Heidelberg Engineering,

Heidelberg, Germany) with automated central macular thickness measurements, generated by using a 19-horizontal line protocol (6- × 6-mm area), each consisting of 1024 A-scans per line. All 39 patients (78 eyes) also underwent customized EDI-SD-OCT scans, consisting of 6- to 9-mm high-resolution line scans through macular/perimacular areas of patchy chorioretinal atrophy; these scans were saved for analysis after up to 100 frames were averaged, using the automatic averaging and eye tracking features of the proprietary device. Fluorescein angiography (FA) using a commercial OCT device (Heidelberg Engineering) and ultrasonography were performed when needed to identify/exclude neovascular complication and to study the relation with the vascular (retinal, choroidal, and scleral/retrobulbar) structures.

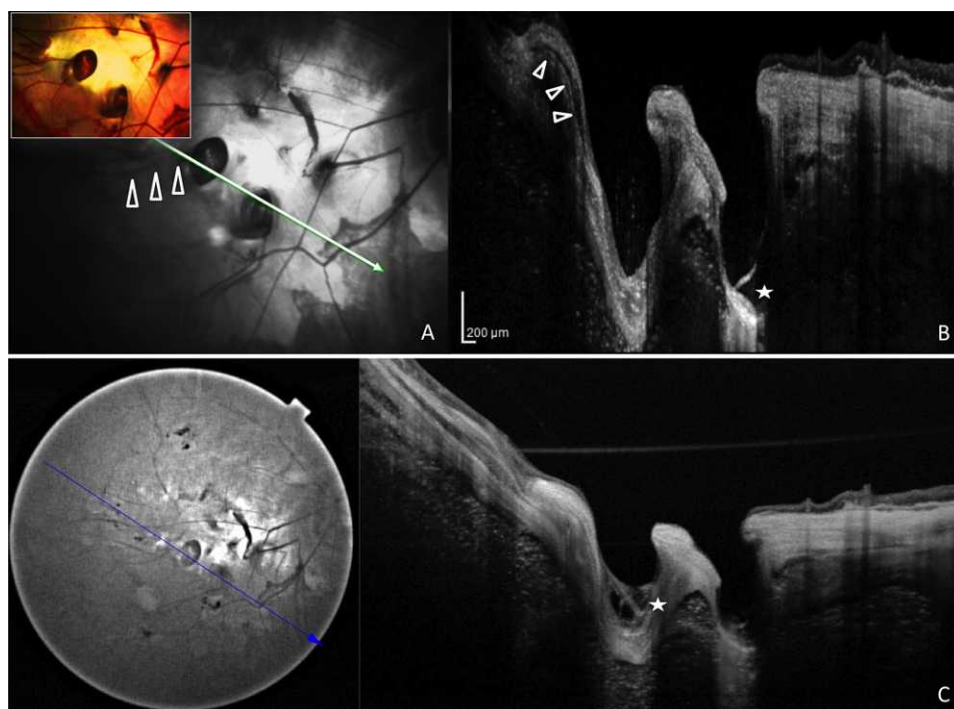


FIGURE 2. Multicolor image, IR, EDI-OCT, and SS-OCT scan of a 68-year-old man with high myopia. IR shows focal scleral ectasia as two deep, dark, round/oval lesions with well-defined borders surrounded by the atrophy crossed by vessels ([A], *open arrowheads*). Note, on multicolor image, large vessels that seem to emerge from the deep dark round/oval lesion. EDI-OCT scan shows one of the vessels running through the sclera at the border of the temporal ectasia ([B], *white arrowheads*). Note the schisis of the retina at the bottom of the ectasia on both EDI-OCT and SS-OCT scans ([B, C], *asterisks*).

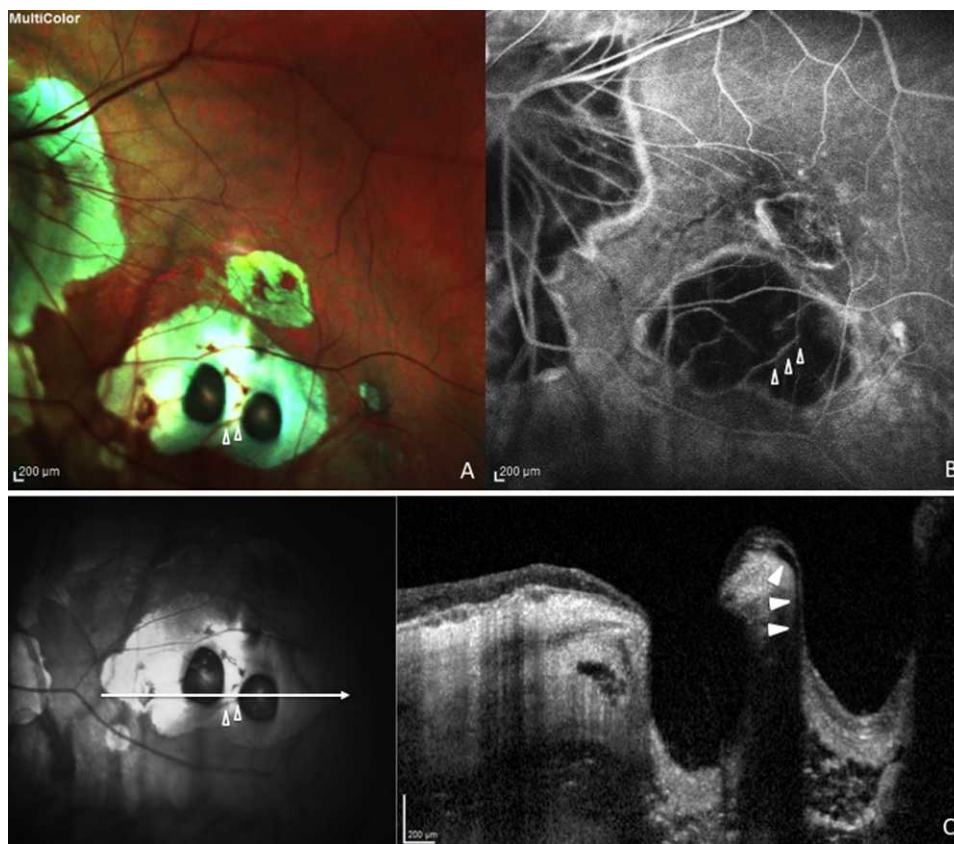


FIGURE 3. Multicolor image, FA, and EDI-OCT of a 79-year-old man with high myopia. Multicolor image (A) shows focal scleral ectasia as two deep, dark, round/oval lesions with well-defined borders surrounded by the atrophy crossed by vessels ([A], *open arrowheads*). On FA, a crossing vessel is visible through the atrophic lesion ([B], *open arrowheads*). EDI-OCT scan shows the vessel perforating the inner sclera at the border of the temporal ectasia ([C], *white arrowheads*).

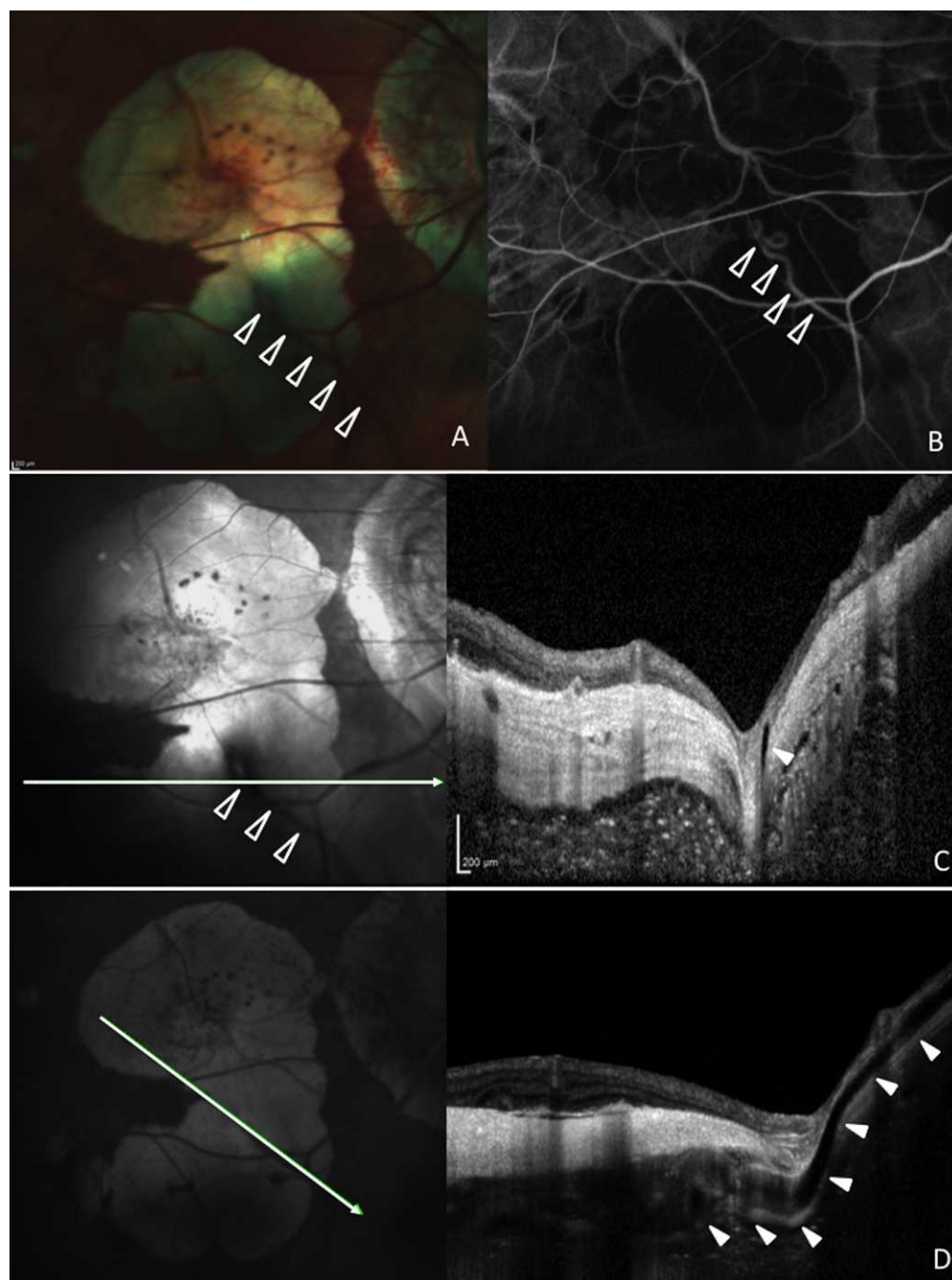


FIGURE 4. Multicolor image, FA, and EDI-OCT of a 65-year-old woman with high myopia. Multicolor imaging shows focal scleral ectasia as a deep, dark, round/oval lesion surrounded by the atrophy crossed by vessels ([A], *open arrowheads*). On FA, a crossing vessel is visible through the atrophic lesion ([B], *open arrowheads*). EDI-OCT scans show the perforating vessel ([C], *white arrowheads*) coming from the retrobulbar space and running through the sclera at the border of the focal ectasia ([D], *white arrowheads*).

Selected patients (13 out of 39 patients, 26 eyes; those that presented after January 2013, date of acquisition of the device from our department) also underwent customized swept-source (SS)-OCT scans (Topcon Corp., Tokyo, Japan) that covered an area of $6 \times 6 \text{ mm}^2$ with up to 256 (horizontal) \times 256 (vertical) B-scan line densities through macular chorioretinal atrophy. Radial scans (12 B-scan lines) were also performed with images made up with 1024 A-scans per line. SS-OCT is a next-generation Fourier-domain OCT, using an SS probe light with a center wavelength of 1040 to 1060 nm, that demonstrates less signal decay over depth compared with

the current SD-OCT, and allows high-penetration imaging of deep retinal tissues such as the choroid and sclera.^{9–11}

csLO multicolor (Heidelberg Engineering) and IR images, and EDI-OCT scans were independently viewed and analyzed with commercial software (Heidelberg Eye Explorer, Spectralis Acquisition and Viewing Modules, version 5.6.1.0; Heidelberg Engineering), by two experienced retinal physicians (GQ, EHS). Presence of focal scleral ectasia in areas of macular/perimacular patchy chorioretinal atrophy, their localization and relation with retinal, choroidal, and retrobulbar vascular structures were recorded. Areas of patchy chorioretinal atrophy around the

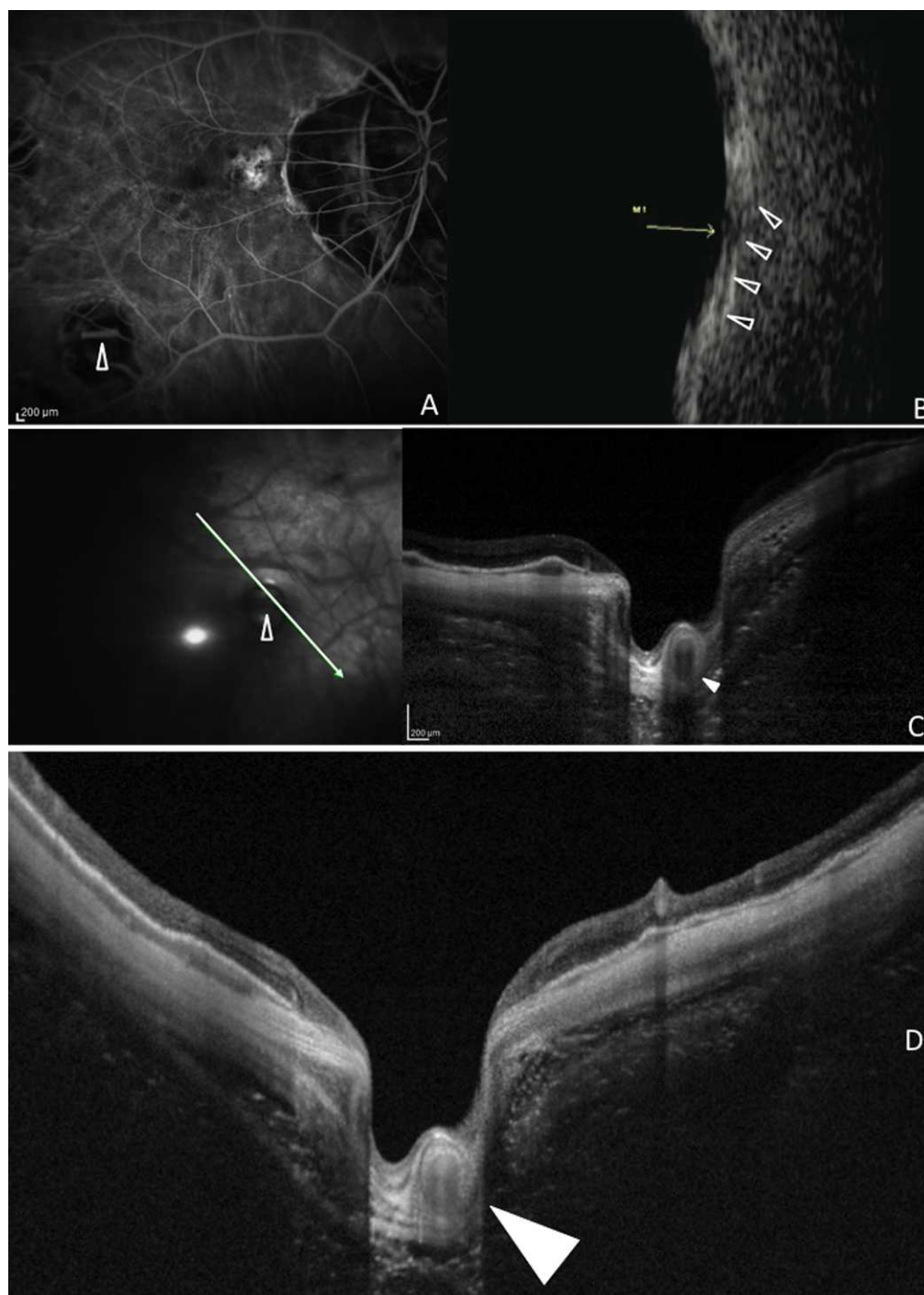


FIGURE 5. Fluorescein angiography ultrasonography, EDI-OCT, and SS-OCT of a 60-year-old woman with high myopia. Fluorescein angiography: a crossing vessel is visible through the atrophic lesion ([A], *open arrowhead*). Ultrasonography shows a vessel coming from the retrobulbar space, and running through the sclera ([B], *open arrowhead*), after being perforated in correspondence of the focal ectasia ([B], *thin arrow*). EDI-OCT (C) and SS-OCT (D) show a cross-section of the perforating vessel at the bottom of the ectasia (*arrowheads*).

optic disc and myopic conus and the recently reported peripapillary pits were not investigated in the current analysis.¹²

Comparisons of mean age and sex in patients with macular/perimacular atrophy showing or not focal scleral ectasia in at least one eye were compared using Student's *t*-test and χ^2 tests, respectively. Mean BCVA (logarithm of the minimum angle of resolution [logMAR]), axial length, and number and size of macular/perimacular patchy atrophy areas, in eyes showing or not showing focal scleral ectasia in at least one eye (in case of

both eyes affected, only one eye was used for statistical calculations), were compared using Student's *t*-test. The chosen level of statistical significance was $P < 0.05$.

RESULTS

A total of 68 eyes of 39 consecutive patients (27 females, 12 males; mean age 65.7 ± 11.9 years [range: 44–87 years]) with

macular/perimacular patchy chorioretinal atrophy were included in the study. Ten eyes were excluded from analysis because of the absence of macular/perimacular patchy chorioretinal atrophy. All patients were Caucasian. Mean BCVA in the study eyes was 0.69 ± 0.67 logMAR. Mean axial length in the study eyes was 31.2 ± 1.61 mm. Mean refractive error in the study eyes was -12.2 ± 2.8 D. Both eyes of 29 patients showed areas of macular/perimacular patchy atrophy (both eyes of 22 patients without focal scleral ectasia, and both eyes of seven patients with focal scleral ectasia). Ten patients showed areas of macular/perimacular patchy atrophy in one eye. The average number of macular/perimacular patchy atrophies was 2.3 ± 1.7 /eye. The mean area of atrophy was 16.7 ± 11.3 mm².

Twelve eyes of 11 patients showed a characteristic focal scleral ectasia (overall 15 scleral ectasia lesions were found) within the area of macular/perimacular patchy atrophy (Figs. 1–5). Focal scleral ectasia, appearing on fundus examination as a deep dark round/oval lesion with well-defined borders surrounded by the atrophy (Figs. 3, 4), was characterized on EDI-OCT by an abrupt posterior bow of the sclera with different degrees of scleral schisis on its borders. The RPE and the choroid were absent in all focal scleral ectasia lesions. In three lesions, there was an almost complete retinal loss overlying focal scleral ectasia (Figs. 1, 3, 5), while in nine focal scleral ectasia lesions, only the outer retina was absent (Figs. 2, 4). In three lesions, there was a retinoschisis appearance overlying focal scleral ectasia (Fig. 2). These same features were also observed in the selected eyes examined with SS-OCT (Figs. 1, 2, 5).

Fifty-six eyes of 34 patients did not show any focal scleral ectasia within the area of macular/perimacular patchy atrophy (50 eyes of 28 patients without focal scleral ectasia in either eye, and six fellow eyes of six patients with unilateral focal scleral ectasia). Ten patients showed focal scleral ectasia in one eye within the area affected with macular/perimacular patchy atrophy. One patient showed, in both eyes, focal scleral ectasia within the area affected with macular/perimacular patchy atrophy. On EDI-OCT, the curvature of the sclera in the area of macular/perimacular patchy atrophy did not differ from that of the neighboring sclera, and the outer retina, the RPE, and the choroid were absent. The number of focal scleral ectasia in an eye ranged from one to two (mean 1.25 ± 0.38).

Age and sex did not significantly differ in patients with macular/perimacular patchy atrophy showing or not focal scleral ectasia (Table).

Mean BCVA, axial length, and number and size of macular/perimacular patchy atrophy areas, did not significantly differ in eyes showing or not showing focal scleral ectasia (Table).

Areas of patchy atrophy were more often located inferior ($72\% = 49/68$), than temporal ($57\% = 39/68$), superior ($47\% = 32/68$), or nasal ($50\% = 34/68$) to the macula.

All focal scleral ectasias were observed, on IR or multicolor imaging (Heidelberg Engineering), inferior or temporal to the macula, often close to the inferior vascular arcade.

Interestingly, cSLO images (Heidelberg Engineering; Figs. 3, 4) and IR reflectance (Figs. 1, 4, 5) showed large vessels that seem to emerge from the deep dark round/oval lesion corresponding to the focal scleral ectasia, and crossing the area of patchy atrophy. In all 15 focal scleral ectasia lesions, EDI-OCT revealed the presence of large vessels on the borders or at the bottom of the abrupt posterior bow of the sclera. When the scans were acquired parallel to the axis of the vessels (5 out of 12 eyes) in areas of patchy atrophy (as visualized by cSLO multicolor [Heidelberg Engineering] or IR reflectance images), EDI-OCT showed retrolbulbar vessels perforating the sclera at the borders/bottom of the abrupt posterior bow of the sclera (i.e., focal scleral ectasia) and

TABLE. Demographics and Clinical Features of Patients With Patchy Atrophy, With and Without Focal Scleral Ectasia

	With Focal Scleral Ectasia	Without Focal Scleral Ectasia	P Value
Sex, <i>n</i>			
Male	4	8	
Female	7	20	0.5*
Age, y, mean \pm SD	69.9 ± 10.5	61.5 ± 13.2	0.2†
LogMAR, mean \pm SD	0.78 ± 0.65	0.61 ± 0.70	0.5†
Axial length, mm, mean \pm SD	30.63 ± 1.19	31.88 ± 2.03	0.1†
Number of patchy atrophy per eye, mean \pm SD	2.2 ± 1.7	2.5 ± 1.6	0.6†
Area of atrophy per eye, mm ² , mean \pm SD	20.1 ± 12.0	13.5 ± 10.6	0.052†

* χ^2 test.

† Student's *t*-test.

running through the superficial scleral thickness for the whole extension of the atrophic area (Fig. 4). Similar findings were detected by SS-OCT in eyes with focal scleral ectasia (six eyes of five patients; Figs. 2, 5). On the other hand, no differences were detected between EDI-OCT and SS-OCT findings in 16 eyes of 10 patients (14 eyes of 8 patients without focal scleral ectasia in either eye, and two fellow eyes of two patients with unilateral focal scleral ectasia) affected with macular/perimacular patchy atrophy without focal scleral ectasia (the curvature of the sclera in the area of macular/perimacular patchy atrophy did not differ from that of the neighboring sclera, and the outer retina, the RPE, and the choroid were absent). The presence of retrolbulbar vessels perforating the sclera at the borders/bottom of the abrupt posterior bow of the sclera (i.e., focal scleral ectasia) and running through the superficial scleral thickness was confirmed by ultrasonography (two eyes of two patients showing focal scleral ectasia within the area affected with macular/perimacular patchy atrophy; Fig. 5). FA, performed in all 11 patients with focal scleral ectasia, did not show any neovascular complication.

DISCUSSION

In this study, we describe the presence of focal scleral ectasia in areas of macular/perimacular patchy atrophy secondary to pathologic myopia, appearing on fundus examination as deep dark round/oval lesions with well-defined borders surrounded by the atrophy. Focal scleral ectasia was found in 11 out of 39 consecutive patients (12 out of 68 eyes) affected by pathologic myopia with macular/perimacular patchy chorioretinal atrophy. Interestingly, age, sex, axial length, number, and size of patchy atrophy did not significantly differ in patients with macular/perimacular patchy atrophy showing or not showing focal scleral ectasia.

On EDI-OCT, focal scleral ectasia was characterized by an abrupt posterior bow of the sclera with different degrees of scleral schisis on its borders. It is noteworthy that the outer retina, the RPE, and the choroid were absent in areas of macular/perimacular patchy atrophy, as well as in focal scleral ectasia. This, together with the deep penetration OCT signal (EDI and SS), allowed visualizing retrolbulbar vessels perforating the sclera at the borders/bottom of the abrupt posterior bow of the sclera (i.e., focal scleral ectasia) and running

through the superficial scleral thickness for the whole extension of the atrophic area.

Why focal scleral ectasia was always observed inferior or temporal to the macula, often close to the inferior vascular arcade, and which kind of vessels was perforating the sclera at its borders/bottom, is not clear. Recently, Ohno-Matsui et al.¹² described structures in the optic disc area—including the area of the conus—of eyes with pathologic myopia, looking very similar to the focal scleral ectasia here reported, which they named “peripapillary pits.” They suggested that the conus pits may develop from a scleral stretch-associated schisis in areas of openings of posterior emissary for the short posterior ciliary arteries in the sclera. Similarly, focal scleral ectasia in areas of macular/perimacular patchy atrophy may develop from a scleral stretch-associated schisis, more pronounced inferiorly (possibly due to oculomotor, gravitational, and staphyloma-associated stretching forces), in areas of openings of anterior emissary for the short posterior ciliary arteries in the sclera.

Differently from the recently described macular intrachoroidal cavitation¹⁵ and focal choroidal excavation,^{14–16} the choroid the RPE and the outer retina are absent in focal scleral ectasia, there are various degrees of thinning/schisis of the inner retina, and there is an exaggerated focal scleral protrusion with an aspect of schisis on its borders.

Our study has several limitations. The series presented here is relatively small. Moreover, we had no examples of histopathology to correlate to the changes noted on EDI and SS-OCT. Finally, current data cannot answer the question of cause-effect relationship. In other words, we cannot definitively conclude whether the focal scleral ectasia and the visualization of the perforating vessels on its borders/bottom are primarily involved in the development of atrophy or if they result from the primary absence of the outer retina, the RPE, and the choroid (patchy atrophy). However, the presence of macular/perimacular patchy atrophy without abrupt posterior bow of the sclera in subjects/eyes presenting similar demographics/myopic characteristics (Table) suggests the latter as the most possible mechanism responsible for focal scleral ectasia development in regions of vessels perforation. In turn, given that the expansion of the sclera should be more pronounced in atrophic areas, when these involve vessels perforation regions, then focal scleral ectasia may develop.

In conclusion, we showed focal scleral ectasia in areas of macular/perimacular patchy atrophy. Perforating vessels are characteristically localized at the borders/bottom of the focal scleral ectasia. Spatial coincidence of patchy atrophy and reduced rigidity of the sclera in regions of vessels perforation, may lead to focal scleral ectasia development.

Acknowledgments

Disclosure: **A. Pedinielli**, None; **E.H. Souied**, None; **F. Perrenoud**, None; **N. Leveziel**, None; **V. Caillaux**, None; **G. Querques**, None

References

1. Morgan IG, Ohno-Matsui K, Saw S-M. Myopia. *Lancet*. 2012; 379:1739–1748.
2. Flores-Moreno I, Lugo F, Duker JS, et al. The relationship between axial length and choroidal thickness in eyes with high myopia. *Am J Ophthalmol*. 2013;155:314–319.
3. Liu HH, Xu L, Wang YX, et al. Prevalence and progression of myopic retinopathy in Chinese adults: the Beijing Eye Study. *Ophthalmology*. 2010;117:1763–1768.
4. Moriyama M, Ohno-Matsui K, Hayashi K, et al. Topographic analyses of shape of eyes with pathologic myopia by high-resolution three-dimensional magnetic resonance imaging. *Ophthalmology*. 2011;118:1626–1637.
5. Ohno-Matsui K, Shimada N, Yasuzumi K, et al. Long-term development of significant visual field defects in highly myopic eyes. *Am J Ophthalmol*. 2011;152:256–265.
6. Hayashi K, Ohno-Matsui K, Shimada N, et al. Long-term pattern of progression of myopic maculopathy. *Ophthalmology*. 2010; 117:1595–1611.
7. Spaide RF, Koizumi H, Pozzoni MC. Enhanced depth imaging spectral-domain optical coherence tomography. *Am J Ophthalmol*. 2008;146:496–500.
8. Invernizzi A, Giani A, Cigada M, et al. Retrobulbar structure visualization with enhanced depth imaging optical coherence tomography. *Invest Ophthalmol Vis Sci*. 2013;54:2678–2684.
9. Hirata M, Tsujikawa A, Matsumoto A, et al. Macular choroidal thickness and volume in normal subjects measured by swept-source optical coherence tomography. *Invest Ophthalmol Vis Sci*. 2011;52:4971–4978.
10. Ikuno Y, Kawaguchi K, Nouchi T, et al. Choroidal thickness in healthy Japanese subjects. *Invest Ophthalmol Vis Sci*. 2009; 51:2173–2176.
11. Esmateelpour M, Povazay B, Hermann B, et al. Three-dimensional 1060-nm OCT: choroidal thickness maps in normal subjects and improved posterior segment visualization in cataract patients. *Invest Ophthalmol Vis Sci*. 2010;51:5260–5266.
12. Ohno-Matsui K, Akiba M, Moriyama M, et al. Acquired optic nerve and peripapillary pits in pathologic myopia. *Ophthalmology*. 2012;119:1685–1692.
13. Ohno-Matsui K, Akiba M, Moriyama M, et al. Intrachoroidal cavitation in macular area of eyes with pathologic myopia. *Am J Ophthalmol*. 2012;154:382–393.
14. Wakabayashi Y, Nishimura A, Higashide T, et al. Unilateral choroidal excavation in the macula detected by spectral-domain optical coherence tomography. *Acta Ophthalmol*. 2009;88:e87–e91.
15. Margolis R, Mukkamala SK, Jampol LM, et al. The expanded spectrum of focal choroidal excavation. *Arch Ophthalmol*. 2011;129:1320–1325.
16. Katome T, Mitamura Y, Hotta F, et al. Two cases of focal choroidal excavation detected by spectral-domain optical coherence tomography. *Case Rep Ophthalmol*. 2012;3:96–103.